EFFECT OF MASS OF THE PRIMARY KNOCK-ON ATOM ON DISPLACEMENT CASCADE DEBRIS IN α-IRON—A. F. Calder, D. J. Bacon, A. V. Barashev (The University of Liverpool), and Yu. N. Osetsky (Oak Ridge National Laboratory)

SUMMARY

Results are presented from molecular dynamics (MD) simulations of displacement cascades created in α-iron (Fe) by primary knock-on atoms (PKAs) with energy from 5 to 20 keV and mass chosen to represent C, Fe and Bi. Molecular Bi_2 has also been simulated using two Bi PKAs, and PKA-Fe interaction potential has also been varied. Four effects are reported. First, the PKA mass has a major effect on cascade damage while the interaction potential has little if any. Second, the total number of point defects produced in a cascade decreases with increasing PKA mass. This fact is not accounted for in models used conventionally for estimating damage. Third, interstitial loops of ½<111> type and both vacancy and interstitial loops of <100> type are formed, the latter being observed in MD simulation for the first time. The probability of <100> loop appearance increases with increasing PKA mass as well as energy. Finally, there is a correlation between production of large vacancy and interstitial clusters in the same cascade.

PROGRESS AND STATUS

Introduction

Degradation of mechanical properties of iron (Fe) and ferritic alloys in nuclear reactors is associated with microstructural changes occurring under neutron irradiation. One of the principal effects is the formation of point defect clusters, which are obstacles to moving dislocations causing radiation the induced strengthening and loss of ductility. Understanding of this process is still poor. For example, the occurrence of interstitial-type loops with the Burgers vector ***b*** = <100> remains unexplained [1,2]. Eyre and Bullough [3] proposed that such a loop can form as a result of ½<1$\bar{1}$0> shear of a faulted ½<110> loop. Molecular dynamics (MD) simulations with existing interatomic potentials have not confirmed this, however. They show that, first, only ½<111> clusters of self-interstitial atoms (SIAs), which are the most stable configuration, are produced in displacement cascades [4]. Second, although rhombus-shaped ½<110> 16-SIA clusters and larger do transform into <100> configuration at temperature T = 0K [5], all clusters, independently of the starting state, transform into ½<111> configuration on simulating T > 0K [5-7]. Another mechanism of a <100> loop formation resulting from coalescence of two ½<111> loops was proposed by Masters [2]. However, it too is not supported by MD simulations because, although segments of <100> type do form due to interaction between two mobile ½<111> clusters, they are unstable and a single ½<111> loop eventually forms [8,9]. In fact, there has been only one reported observation of the formation of a <100>-type vacancy loop by Soneda et al. [10] and none of interstitial type. Soneda et al. ran a hundred 50 keV PKA cascades to detect one such event, which indicates that it is rare and perhaps more probable in high energy cascades.

Many experimental studies have been reported that use either self-ion or heavy-ion irradiation of thin foils to simulate bulk damage from neutrons and investigate the effects of cascade parameters on damage. Although there are problems in interpretation of the results due to proximity of surfaces and resolution limit of the transmission electron microscope (TEM), there are clear trends for α-iron. For example, Jenkins et al. [11] have shown that self-ion irradiation does not result in visible damage up to the dose level where cascade overlap is significant. Further, an increase of the incident ion mass increases the defect yield, i.e., the number of visible loops formed per incident ion after irradiation to the same dose level, and also leads to an increase of the mean loop size. (We use the term 'loop' here to refer to a cluster of point defects that creates diffraction contrast consistent with a dislocation loop.) Loops with Burgers vector ***b*** of ½<111> and <100> type have been observed, both are reported to be of vacancy type. Thus, there is clearly an effect of varying ion type in defect production in cascades, while simple models conventionally used to estimate the damage, e.g., NRT standard [12], are insensitive to the ion nature.

To the best of our knowledge, the effect of PKA mass on displacement cascades has not been studied systematically by MD and is the subject of the present report.

Simulation Method

A simulation box with periodic boundary conditions at a temperature of 600K was used. It was maintained at a constant volume with the lattice parameter a_0 corresponding to zero-pressure conditions at a given temperature before introduction of a PKA. The inter-atomic interaction was described using an embedded-atom-method-type (EAM) empirical potential developed recently with a specific emphasis on a correct description of the relative stability of <111>, <110> and <100> configurations of self-interstitial atoms and the vacancy migration energy [13]. In particular, the formation energy of the <110> dumbbell is ~0.5 eV lower than that of a <111> crowdion with this potential, cf. 0.7 eV obtained ab initio [14], and the <110> configuration is more stable with respect to the <111> for clusters of up to four SIAs. PKA energy of 5, 10 and 20 keV was considered. The size of the model system depended on the PKA energy, being 250 000 for 5 keV, 500 000 for 10 keV and 2 000 000 for 20 keV. No temperature control was applied and the temperature increase due to introduction of the PKA in the corresponding simulations was approximately 60, 70 and 30K, respectively. The integration of equations of motion was performed using a leapfrog algorithm with a variable time-step, determined by a fixed value for the displacement of the fastest atom in the system, typically ~$0.003a_0$.

The calculations were performed to simulate cascades in bulk iron with one of three different PKAs: C, Fe, Bi and one molecular Bi_2. In the latter case, two nearest atoms of the lattice were used as the PKA atoms with the same direction and the same energy, equal to half the total energy. The potential for the PKA-Fe interaction was the same as for Fe-Fe over most of the range of atom-atom spacing, but at short range (≤ 0.1 nm), well below the nearest-neighbour spacing, the Universal screened-Coulomb potential [15] for the required atomic pair was used for the pair part of the potential. The two potentials were joined smoothly by an exponential spline over the range 0.100-0.205 nm. Two sets of simulations were performed to elucidate whether PKA mass or interaction potential was primarily responsible for the effects observed. This was done by changing either the mass or potential whilst retaining the other property as that for an Fe atom. The combinations studied and the notation used later for identifying them are summarised in Table 1. The statistics of up to 30 cascade events for each set of conditions (temperature, PKA energy, mass and potential) was accumulated. Independence of calculations was provided by using different <123> and <135> type PKA direction, as well as by introducing the PKA at different times for different atoms.

Table 1. Summary of the number of cascades modelled for each cascade energy for the combinations of PKA mass and PKA-Fe interatomic potential considered. The notation is used in subsequent figures.

PKA (Mass, amu)	C (12.0)	Fe (55.8)	Bi (209.0)	Fe (55.8)	Bi (209.0)	Bi_2 (418.0)
PKA-Fe potential	Fe-Fe	Fe-Fe	Fe-Fe	Bi-Fe	Bi-Fe	Bi-Fe
Notation	C^{Fe}	Fe^{Fe}	Bi^{Fe}	Fe^{Bi}	Bi^{Bi}	Bi_2^{Bi}
5 keV	30	30	30	30	30	-
10 keV	30	30	30	30	30	-
20 keV	30	30	30	-	30	21

MD Results

The dependence of the mean value of the total number, N_F, of either vacancies or SIAs produced in a cascade on the PKA mass for different PKA energy is presented in Fig. 1. Empty symbols are from modelling when only mass of the PKA was changed, while full symbols represent results produced with the Bi-Fe interaction potential for the PKA-Fe pair. The bars are the standard error. It can be seen that within statistical uncertainty, N_F for a given mass does not depend on the PKA-Fe interatomic potential. In contrast, N_F decreases with increasing mass across the mass range 12 to 209 amu for 5 and 10 keV cascades, but only decreases between 12 and 56 amu at 20 keV. For all PKA types, the number of defects increases approximately linearly with PKA energy, a trend similar to that observed previously, e.g., in [16]. An increase of PKA mass also leads to an increase in variability of N_F over different cascades and this effect is particularly strong for heavy PKAs. This is demonstrated by the histogram for the 20 keV simulations in Fig. 2. For example, as seen from Fig. 2, N_F ranges from 4 to 82 in the 21 cascades created by Bi_2 PKAs, compared with 26 to 63 in 30 cascades by Fe PKAs.

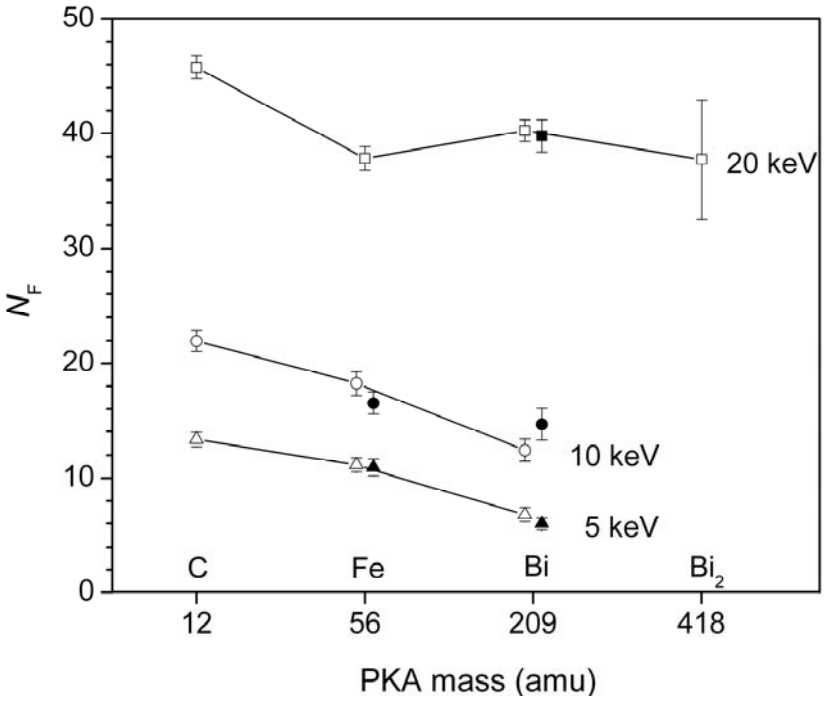

Fig. 1. Dependence of the mean value of the total number, N_F, of either vacancies or SIAs produced in a cascade on the PKA mass for different PKA energy. Empty symbols are for simulations when only mass is changed, while full symbols are for calculations with the Bi-Fe interaction potential for the PKA-Fe pair.

The finding that the PKA mass has a significant effect on defect production is at variance with simple binary collision approximation (BCA) used conventionally to estimate the damage, e.g., the NRT standard [12]. In the absence of inelastic effects, which is the situation in the MD modelling, the NRT number is independent of mass. Furthermore, when electronic energy loss is allowed for, BCA actually predicts a decrease in N_F with decreasing atomic number, which is contrary to the mass effect due to elastic collisions found in the present study.

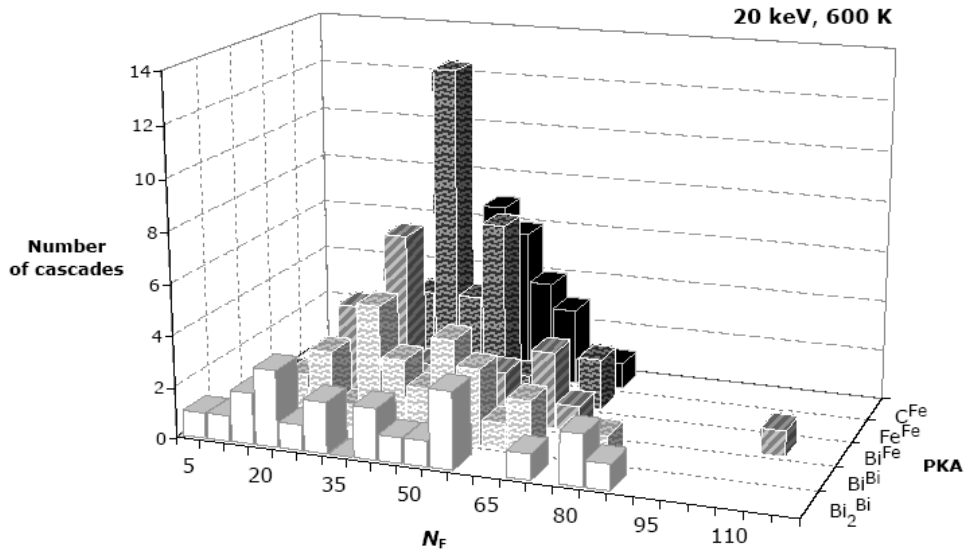

Fig. 2. Distribution of cascades creating N_F defects in the simulations for each type of 20 keV PKA.

Figure 3(a) shows the mass dependence of the fractional population distribution of vacancies as a function of cluster size for all cascades of 20 keV. A cluster is defined such that every vacancy has at least one other vacancy in a nearest-neighbour site. The histogram bin width is 5, except for small size where the first two bins are for defects of size 1 and 2-5, respectively. It is seen that the size distribution broadens with increasing mass, resulting in an increase of the mean cluster size and the creation of larger clusters by the Bi and Bi_2 PKAs. This is qualitatively consistent with TEM observations by Jenkins *at al*. of vacancy loops produced by cascade collapse in iron [11]. The fraction of vacancies created in clusters is also affected by PKA mass, for the fraction of singles decreases from approximately 0.6-0.7 for C and Fe PKAs to around 0.4 for the heavier PKAs.

Similar trends with increasing PKA mass are found in the distribution of clustered interstitials, as can be seen from the data for 20 keV plotted in Fig. 3(b). Here, the influence on the total clustered fraction is particularly strong, for the fraction of single SIAs falls from 0.6 for C to 0.1 for Bi_2.

Interstitial loops of ½<111> type and both vacancy and interstitial loops of <100> type were formed in these simulations. Clusters of the first type are commonly found in MD studies of displacement cascades in α-Fe, even for energy of only a few keV (see, e.g., [4]), but <100> loops are not. As noted in section 1, the only observation reported previously was by Soneda et al. [10], who found one <100> vacancy loop in the damage of one hundred simulations of 50 keV cascades created by Fe PKAs.

Examples of the <100> dislocation loops in the present work are presented in Figs. 4(a) and (b). They show atoms (solid circles) in two (001) planes through the centre of loops with ***b*** = [100]: isolated single vacancies are shown as empty squares in Fig. 4(a). The lines are added to aid visualisation of the distortion around the loops. The clusters in Figs. 4(a) and (b) contain 57 vacancies and 30 SIAs, respectively. Each loop formed directly in the cascade process by the creation of vacancies or SIAs on two adjacent (100) atomic planes.

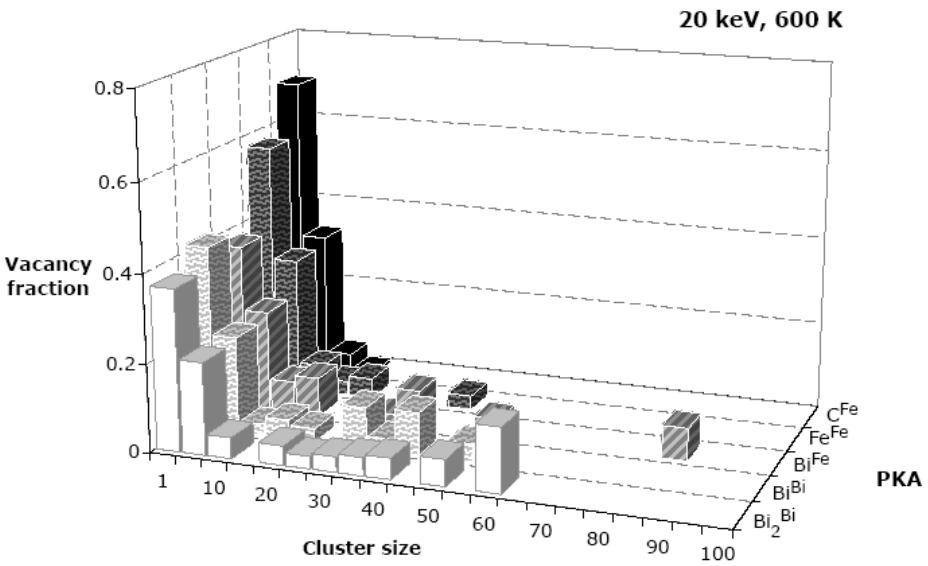

(a)

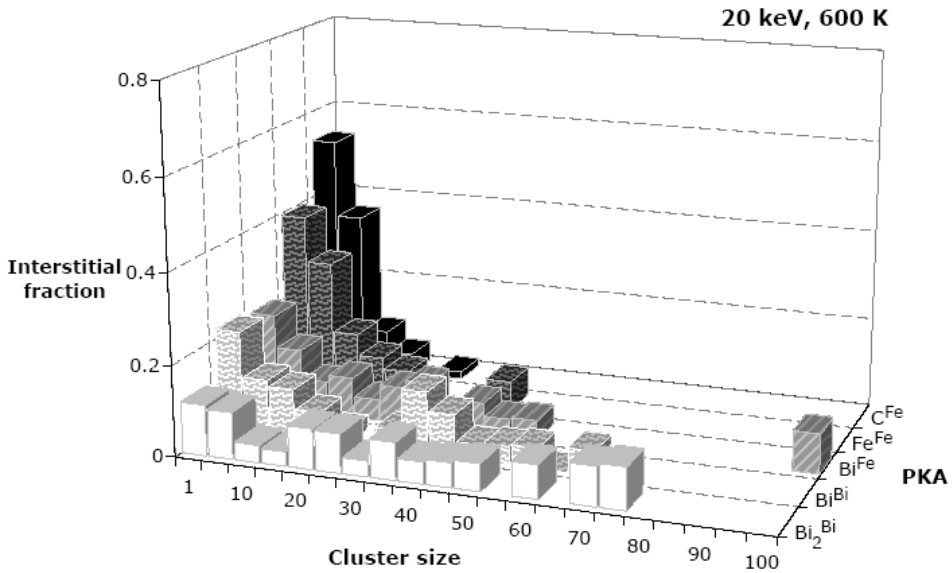

(b)

Fig. 3. Variation of population fraction with cluster size for the 20 keV simulations for each type of PKA: (a) vacancies and (b) SIAs.

No clusters with <100> loop morphology were found in cascade damage created by C and Fe self-ion PKAs. The <100> interstitial defect in Fig. 4(b) is the only one of this type found in all the simulations. It is the first of its kind created in simulation and was formed when molecular Bi_2 irradiation was mimicked by two Bi PKAs. <100> vacancy loops are more common, for six examples were found in 20 keV cascades: two out of 60 simulations with a Bi PKA and four out of 21 with Bi_2. It is clear, therefore, that the probability of <100> cluster formation increases with increasing PKA mass as well as energy. Note that clusters reported above are ~2 nm diameter, implying that the defects observed in TEM experiments can be produced directly in cascades.

Recent MD simulations of cascades in zirconium [17] and copper [18] have revealed a correlation in the production of interstitial and vacancy clusters, in that cascades with a high proportion of vacancies in clusters are more likely to have a high proportion of clustered interstitials. The results obtained here for iron support this. Furthermore, a correlation exists not only for the cluster fractions but also the size of the clusters. This correlation is clear in Fig. 5, where the maximum size of a vacancy cluster is plotted against the largest SIA cluster produced in the same cascade for the 20 keV simulations. For cascades created by C and Fe PKAs, and those created by heavier PKAs but with only small clusters, most data points fall below the line drawn at 45°, reflecting the difference in the vacancy and interstitial cluster size distribution seen in Figs. 3(a) and (b). For heavy PKAs, there is still a spread of points below the 45°line, but with a tendency to lie near it with increasing cluster size.

Discussion

As has already been mentioned in the Introduction, TEM analysis of loop images in iron foils irradiated to low dose provides evidence that the damage from self-ions differs from that due to heavy ions. The former does not result in visible damage up to the dose level where cascade overlap is significant [11], while the latter produces <100> vacancy-type loops. The situation is different in bulk samples irradiated by neutrons to a similar NRT dose level. In this case, the PKAs are Fe atoms and the damage might be expected to be comparable to that for self-ion irradiation. Although visible defect clusters do form under neutrons, they are of interstitial-type with ***b*** equal to either ½<111> or <100> (see [19] and references cited therein).

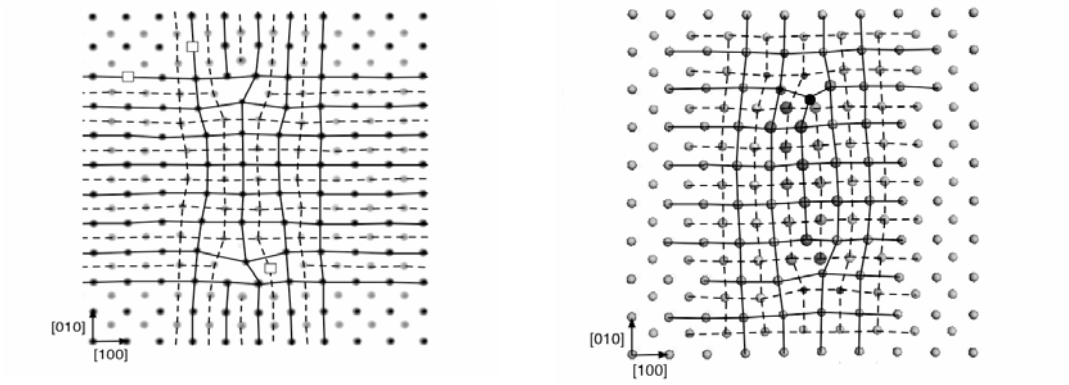

(a) (b)

Fig. 4. (a) Cross section through a vacancy cluster of <100> type containing 57 vacancies. (b) Cross section through an interstitial cluster of <100> type containing 30 SIAs.

On the basis of the present work it is possible to speculate on the link to experiments as follows. With regard to the vacancy component of damage, the MD simulations are in agreement with experiment that the Burgers vector of vacancy loops produced in cascades is <100> rather than ½<111>, despite the fact that the formation energy of the latter is lower [14]. Furthermore, the probability of vacancy loop formation increases with increasing PKA mass and is very small for Fe PKAs. Hence, there is satisfactory correspondence between the modelling and the observed vacancy component of damage in both the bulk and TEM foils. For the interstitial component, the MD simulations predict, and neutron irradiation experiments reveal, the formation of a high density of ½<111> SIA clusters in the bulk of iron and much smaller probability of <100>-type cluster formation. The absence of SIA clusters in ion-irradiated foils is believed to be due to the free surfaces acting as efficient sinks for ½<111> SIA clusters, which are highly mobile [6]. This annihilation increases the vacancy population left in the foil in both single and clustered form, which also acts as recombination centres for the SIA clusters. These processes suppress survival and growth of SIA loops in foils with respect to the bulk of iron, where the density of annihilation centres for SIA clusters is lower. Nevertheless, there does not seem to be an obvious reason why a fraction of <100> loops, however small, in heavy-ion irradiated iron foils should not have interstitial nature and it is hoped that experiments known to be underway in several laboratories may confirm or disprove this conjecture.

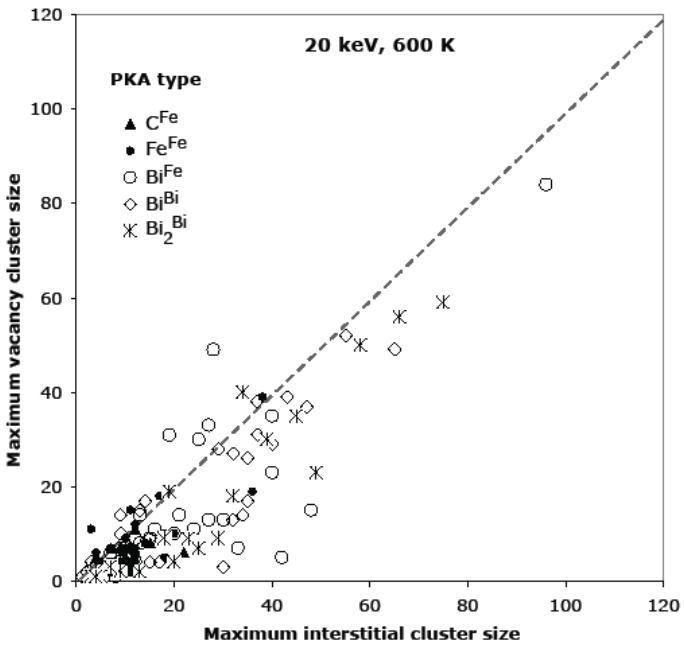

Fig. 5. Maximum size of a vacancy cluster versus that of an SIA cluster produced in the same cascade for 20 keV PKA simulations.

The question arises as to why the probability of <100> loop formation increases with increasing PKA mass, both in experiment and MD simulation. In order to explain the former, it has been argued on the basis of binary-collision estimates that, although N_F is independent of PKA mass, the cascade volume decreases with increasing mass [11,20]. Thus, higher energy and vacancy density is achieved, and this results in a higher probability of cascade collapse and loop formation. This was supported by the first MD simulations of collapse by Matthai and Bacon [21], who used a pair wise interatomic potential to simulate a small void placed in the zone of a thermal spike and found that an extended dislocation defect, namely a loop in iron and a stacking fault tetrahedron in copper, was formed during the spike lifetime. Interestingly, the loop in iron was of <100> type, even though a ½<111> loop with the same number of vacancies has lower formation energy. Kapinos et al. [22, 23] also showed by MD modelling that conditions of high energy and vacancy density favour collapse to vacancy dislocation loops in metals. Observations made in the present work are qualitatively consistent with this. As an illustration of this, in Fig. 6 we plot the variation with PKA mass of the mean value of the maximum number, N_{max}, of atoms displaced from a lattice site by more than $0.3a_0$ in a 20 keV cascade and the mean of the time, t_{max}, at which this maximum is reached. As can be seen, the higher the PKA mass the higher the number of atoms displaced from their original position. This is an indication, however indirect, of localisation of the cascade energy both in space and time. It seems probable that a corresponding decrease in the final defect yield might be just a consequence of closer proximity of the vacancy and interstitial in cascades produced with heavier PKA, and hence a more efficient recombination process.

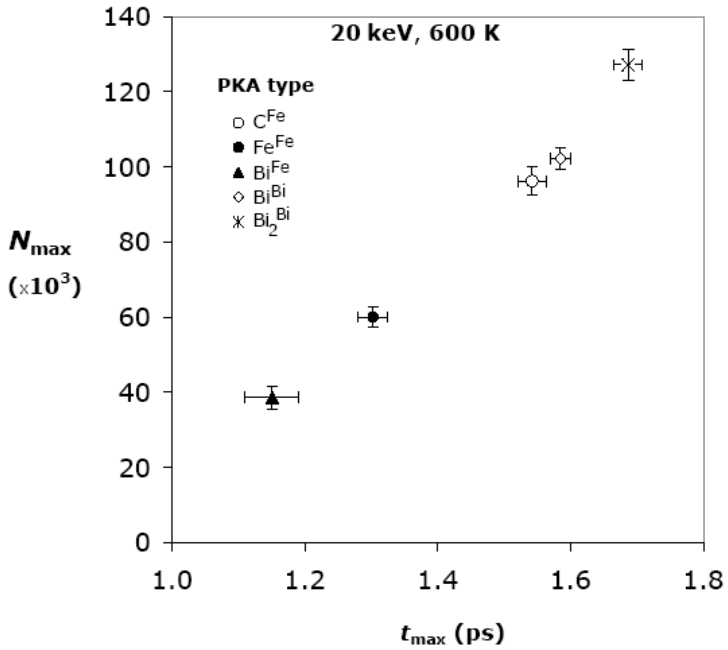

Fig. 6. Variation with PKA mass of the mean value of the maximum number, N_{max}, of atoms displaced by ≥ $0.3a_0$ in a 20 keV cascade and the mean of the time, t_{max}, at which this maximum is reached.

Conclusions

1) The PKA mass has a major effect on cascades while the interaction potential has little if any.
2) The total number of point defects produced in a cascade decreases with increasing PKA mass, and the effect is stronger for lower PKA energy. This fact is not accounted for in the binary-collision models.
3) In addition to usual the ½<111>-type SIA loops, one <100> SIA loop has been observed for the first time in MD, when simulating molecular Bi irradiation.
4) <100> vacancy loops have been observed with heavier PKAs.
5) With heavier PKA the cluster size is bigger and the probability of <100> cluster formation increased. This correlates with the observations by Jenkins *at al*. [11].
6) Strong correlation between the maximum size of a vacancy and an SIA cluster produced in the same cascade has been established.

References

[1] B. L. Eyre and A. F. Bartlett, Philos. Mag. 12 (1965) 261.
[2] B. C. Masters, Philos. Mag. 11 (1965) 881.
[3] B. L. Eyre and R. Bullough, Philos. Mag. 12 (1965) 31.
[4] A. F. Calder and D. J. Bacon, J. Nucl. Mater. 207 (1993) 25.
[5] K. Tapasa et al., J. Nucl. Mater. 361 (2007) 52.
[6] Yu. N. Osetsky et al., Philos. Mag. 83 61 (2003).
[7] B. D. Wirth et al., J. Nucl. Mater. 244 (1997) 185.
[8] Yu. N. Osetsky, A. Serra, and V. Priego, J. Nucl. Mater. 276 (2000) 202.
[9] J. Marian, B. D. Wirth, and J. M. Perlado, Phys. Rev. Lett. 88 (2002) 255507.
[10] N. Soneda, S. Ishino, and T. Diaz de la Rubia, Philos. Mag. Lett. 81 (2001) 649.
[11] M. L. Jenkins, C. A. English, and B. L. Eyre, Philos. Mag. 38 (1978) 97.
[12] M. J. Norgett, M. T. Robinson, and I. M. Torrens, Nucl. Eng. Des. 33 (1975) 50.
[13] G. J. Ackland et al., J. Phys.: Condens. Matter 16 (2004) S2629.
[14] F. Willaime et al., Nucl. Instrum. Methods Phys. Res., Sect. B 228 (2005) 92.
[15] J. P. Biersack and J. F. Ziegler, Nucl. Instrum. Methods Phys. Res. 194 (1982) 93.
[16] D. J. Bacon, Yu. N. Osetsky, R. Stoller, and R. E. Voskoboinikov, J. Nucl. Mater. 323 (2003) 152.

[17] R. E. Voskoboinikov, Yu. N. Osetsky, and D. J. Bacon, Journal of ASTM International 2, paper JAI12410 (2005).
[18] R. E. Voskoboinikov, Yu. N. Osetsky, and D. J. Bacon, Journal of Nuclear Materials (submitted).
[19] S. J. Zinkle and B. N. Singh, J. Nucl. Mater. 351 (2006) 269.
[20] C. A. English and M. L. Jenkins, Mater. Sci. Forum 15-18 (1987) 1003.
[21] C. C. Matthai and D. J. Bacon, J. Nucl. Mater. 135 (1985) 173.
[22] V. G. Kapinos, Yu. N. Osetsky, and P. A. Platonov, J. Nucl. Mater. 170 (1990) 66.
[23] V. G. Kapinos, Yu. N. Osetsky, and P. A. Platonov, J. Nucl. Mater. 173 (1990) 229.